Biosensors and Bioelectronics 38 (2012) 11–18

Contents lists available at SciVerse ScienceDirect

Biosensors and Bioelectronics

journal homepage: www.elsevier.com/locate/bios

CuO thin film based uric acid biosensor with enhanced response characteristics

Kajal Jindal [a], Monika Tomar [b], Vinay Gupta [a,*]

[a] Department of Physics and Astrophysics, University of Delhi, Delhi 110007, India
[b] Department of Physics, Miranda House, University of Delhi, Delhi 110007, India

ARTICLE INFO

Article history:
Received 10 January 2012
Received in revised form
21 March 2012
Accepted 29 March 2012
Available online 20 April 2012

Keywords:
Uric acid
Copper oxide
Thin film
Pulsed laser deposition
Biosensor

ABSTRACT

An efficient reagentless uric acid biosensor has been realized using a copper oxide (CuO) thin film matrix grown onto platinum (Pt) coated corning glass substrates by pulsed laser deposition (PLD) technique. The p-type CuO matrix successfully introduces redox property in the electrode and provides enhanced electron communication features. Sensing response obtained by the bioelectrocatalytic oxidation of uric acid by uricase/CuO/Pt/glass electrode was studied without any external mediator using cyclic voltammetry (CV) and photometric assay. The studies reveal that the uricase/CuO/Pt/glass bio-electrode exhibits good linearity over a wide range of 0.05 mM to 1.0 mM uric acid concentration with enhanced response of 2.7 mA/mM and high shelf life (> 14 weeks). A low Michaelis–Menten constant (K_m) of 0.12 mM, indicate that the immobilized enzyme (uricase) has enhanced affinity towards its analyte (uric acid). The results confirm promising application of the p-type CuO thin film matrix for the realization of a reagentless integrated implantable biosensor.

1. Introduction

It is a growing requirement to develop new methodologies for easy, selective, accurate and reliable quantification of the important metabolites to be used as an index for the state of health in these years. Uric acid (UA) is a chief nitrogenous component of biological fluids such as urine and blood serum. It is one of the primary end products of purine metabolism in human body and can be used as a potent indicator for an early warning sign of numerous illnesses and physiological disorders. The physiological normal level of uric acid in human blood is between 0.13 and 0.46 mM (Luo et al., 2006; MedlinePlus: NLM). Abnormal levels of UA in the blood is a symptom of a number of diseases such as gout, hyperuricemia or Lesch–Nyhan syndrome, arthritis, diabetes, high cholesterol, renal, neurological, cardiovascular and kidney diseases. Thus, detection of UA level dissolved in human physiological fluids is indispensable for the diagnosis of patients suffering from these disorders associated with altered purine biosynthesis and catabolism.

Amongst various methods used to detect uric acid, biosensors based on electrochemical detection methods are known to be the most popular because a low detection limit, high selectivity and sensitivity can be easily acquired where matrix plays an important role. Various matrices have been reported to immobilize uricase for the analysis of uric acid, such as cellulose acetate membrane (Gilmartin and Hart, 1994), polyaniline-deposited Pt electrode (Kan et al., 2004), polypyrrole and polyaniline film (Arslan, 2008), chitosan membrane (Perez et al., 2003), polystyrene membrane (Wang and Hagiwara, 2007), ZnO nano tetrapods (Wang et al., 2008), Ir-modified carbon electrode (Luo et al., 2006), polypyrrole film on Pt surface (Cete et al., 2006), ZnO nanorods-modified glassy carbon (GC) electrode (Zhang et al., 2004), and polyaniline/carboxylated multiwalled carbon nanotubes (c-MWCNTs) deposited on ITO-coated glass plate (Bhambi et al., 2010) and so on. A brief comparison of the matrices used for uric acid detection is summarized in Supplementary Table 1. It may be seen that most of the bioelectrodes suffer from certain problems in uric acid determination such as time-consuming sample preparation involving multiple steps, cumbersome fabrication of the bioelectrode based on crosslinkers, which exhibited lack of stability, a poor linear detection range, thereby limiting their application in development of uric acid biosensors. Also, the continuous monitoring of the metabolites for integrated biosensors requires the development of reagentless biosensors that are free from free diffusing redox mediators (Alkire et al., 2011) which can be accomplished by the direct attachment of the mediator onto the electrode. However, the mediator may suffer from the problem of leaching out and requires the attachment of mediator onto the electrode via covalent bonding. The CuO thin film matrix employed in the present work is based on its own redox property providing self mediation for electron transfer from enzyme to the electrode and alleviates the problems in external mediator based reagentless biosensor. Thus, it is important to simplify the detection system for superior catalytic properties for fast, sensitive, and stable detection of uric acid which still poses a challenge for researchers.

* Corresponding author.
E-mail address: vgupta@physics.du.ac.in (V. Gupta).

0956-5663/$ - see front matter © 2012 Elsevier B.V. All rights reserved.
http://dx.doi.org/10.1016/j.bios.2012.03.043

Therefore, metal oxide based thin film matrices have recently gained significant attention due to their biocompatibility, simplicity, high reliability, sensitivity, selectivity, low detection limit, low cost and compatibility for miniaturization etc. (Saha and Gupta, 2011; Saha et al., 2009a, 2009b, 2010; Singh et al., 2007). Amongst different metal oxides that have been exploited as an efficient electrode for biosensing, copper oxide (CuO), an important p-type semiconductor metal oxide with a narrow band gap (1.2 eV) is of immense interest as a matrix in biosensors with virtue of natural abundance, low cost, non-toxic, good electrochemical activity i.e catalytic effect resulting from the multi-electron oxidation, high isoelectric point (IEP$\sim$9.5) and the possibility of promoting electron transfer reactions at a lower potential resulting in direct electro-oxidation of uric acid. High IEP of CuO is advantageous in immobilization of enzymes having low IEP by physical adsorption technique on the surface of the matrix. Furthermore, CuO has its own redox couple i.e it provides direct electron transfer between the redox protein and electrode, which thus paves the way towards the fabrication of reagentless bio-electrode providing electron transfer pathway through the developed biosensor. There are few reports on using CuO nanostructures and its composites, prepared by chemical route in glucose (Wang et al., 2010) carbohydrates and hydrogen peroxide biosensing (McAuley et al., 2008) due to its good stability and electrocatalytic properties but reproducibility, stability of the matrix are still major concerns and needs to be overcome. To the best of our knowledge, no effort has been made towards the development of CuO thin film based bio-electrode using physical deposition techniques such as pulsed laser deposition (PLD) and rf-sputtering, which are known to be preferred for reproducible and stoichiometric growth of thin films at low temperatures which are compatible with solid state devices for applications in implantable biosensor. In this work, a highly stable laser ablated CuO thin film based bio-electrode has been developed for the fabrication of reagentless uric acid biosensor having efficient biosensing response characteristics.

2. Experimental

2.1. Reagents

Uric acid (99.99% pure), Uricase, horseradish peroxidase (HRP), o-dianisidine dye were procured from Sigma-Aldrich. Sodium phosphate monobasic anhydrous and sodium phosphate dibasic dihydrate were obtained from Sisco chemical, India. All chemicals were of analytical reagent grade and were used without further purification. All the aqueous solutions were prepared using deionized water. A 50 mM phosphate buffer saline (PBS) solution was freshly prepared by mixing solutions of monosodium dihydrogen phosphate and disodium hydrogen phosphate containing 0.9% sodium chloride. The pH of the prepared solution was 7. Enzyme solutions (1 mg/ml) having 4.9 units of uricase were prepared by dissolving the enzyme in the PBS solution.

2.2. Preparation of CuO thin film based electrode

CuO thin films were grown by Pulsed laser Deposition technique using the fourth harmonic of Continuum Nd:YAG laser at a λ=266 nm onto platinum (Pt) coated corning glass (Pt/glass) substrates to obtain the sensor electrodes. The Pt coating ($\sim$100 nm thick) on corning glass was accomplished using RF-sputtering technique under 100% Ar gas ambient using Pt metal target (99.99% pure). It is found that the adhesion of Pt on corning glass substrate is very poor. Hence, a buffer layer of Ti ($\sim$10 nm) was coated onto the glass substrate using a metallic Ti (99.99% pure) target prior to Pt deposition. CuO thin films ($\sim$110 nm) were deposited by ablating a metal copper target (99.999% pure) in oxygen rich ambient (50 mTorr) at a fluence of 1.2 J/cm^2 and a repetition rate of 10 Hz. The deposition chamber was evacuated to a base pressure of 2×10^{-6} Torr, prior to the deposition. The CuO films were deposited at a substrate temperature of 300 °C and target to substrate distance of 4 cm was maintained. Typical deposition conditions for both Pt/Ti bilayer and CuO thin film using RF sputtering and pulsed laser deposition technique, respectively, are mentioned in Supplementary Table 2.

2.3. Fabrication of uricase/CuO/Pt/glass bio-electrode

In order to prepare the uric acid bio-electrode, 20 μl (0.09 U) of the freshly prepared uricase solution (1 mg/ml in PBS solution) is drop casted on the CuO/Pt/glass electrode at room temperature. It was further kept incubated at 4 °C overnight so that uricase is immobilized electrostatically onto CuO matrix via physical adsorption technique. Thereafter, the prepared bio-electrode (uricase/CuO/Pt/glass) was extensively rinsed with buffer to remove any excess loosely bound uricase. The bio-electrode was dried under nitrogen flow and kept at 4 °C when not in use.

2.4. Experimental characterization

2.4.1. Electrochemical

To study the electrochemical properties of the bio-electrode, cyclic voltammetric measurements were carried out using a Potentiostat/ Galvanostat (Gamry Inc. 600) having a three-electrode electrochemical cell configuration with Ag/AgCl serving as reference electrode, platinum foil as counter electrode and uricase/CuO/Pt as working electrode. 10 ml of phosphate buffer saline (PBS) solution (50 mM, 0.9% NaCl) was used as the electrolyte in electrochemical cell without any mediator.

2.4.2. Optical

Optical properties of the prepared uricase/CuO/Pt/glass bio-electrode were studied using a UV–visible spectrophotometer (Perkin Elmer lambda 35) in order to determine the apparent enzyme activity of the bio-electrode. For photometric assay, uricase/CuO/Pt/glass bio-electrode was dipped in 3 ml PBS solution containing HRP solution (1 mg/ml), 20 μl solution of o-dianisidine dye (1% in H_2O) (freshly prepared) and different concentrations of uric acid solution. After 2 min of incubation of bio-electrode, absorbance corresponding to the oxidation of o-dianisidine, was measured at fixed λ=500 nm for monitoring the enzyme kinetics.

2.4.3. Structural and surface morphological

The crystalline structure and phase of the prepared CuO thin film was characterized by X-ray Diffraction (XRD) technique (Bruker D8). The film thickness was measured using a surface profiler (Dektak 150A). The surface morphology and stretching bonds of the prepared CuO/Pt/glass electrode and uricase/CuO/Pt/glass bio-electrode were investigated using atomic force microscopy (AFM) (Veeco DICP2) and FTIR spectrophotometer (Perkin Elmer; Model Spectrum BX) respectively.

3. Results and discussion

3.1. XRD studies

XRD pattern of the CuO thin film deposited on corning glass substrate at a temperature of 300 °C is shown in Supplementary Fig. 1. Well defined reflection peaks corresponding to (110), (002) and (111) planes of CuO were observed for the deposited thin

films and are in good agreement to the corresponding values reported for the monoclinic crystal structure of copper oxide (JCPDS File no. 5-0661, 1991), indicating that the as-deposited films are single phase and polycrystalline. Average crystallite size was calculated from (111) peak using the Debye Scherrer's formula and is found to be about 11 nm.

3.2. FTIR studies

The as-deposited CuO thin film and uricase immobilized CuO thin film were grown on Si substrates and characterized by the Fourier transform infrared (FTIR) spectroscopy in transmission mode. The corresponding spectra are shown in Fig. 1. FTIR spectra of the CuO thin film shows strong absorption bands at around 420, 442, 480, 508 and 606 cm^{-1} (Fig. 1(a)). The mode at 420 cm^{-1} confirmed the formation of monoclinic CuO phase (Vaseem et al., 2008). The high-frequency mode at 606 cm^{-1} is reported to be a Cu–O stretching vibration along the [$\bar{1}$01] direction and the mode at 508 cm^{-1} is related to Cu–O stretching vibration along [101] direction (Kliche and Popovic, 1990). In addition, observed modes at 442 and 480 cm^{-1} also corresponds to the vibrational bands of CuO (Balamurunga and Mehta, 2001). In the FTIR spectra of uricase/CuO/Pt bio-electrode (Fig. 1(b)), absorption bands at 990, 1085, 1652 and 3289 cm^{-1} are observed which corresponds to C–H bonding of alkene, C–N vibrations, amide linkage of enzyme and O–H stretching respectively, confirming the effective immobilization of uricase on CuO/Pt electrode. It is important to note that on uricase immobilization, modes corresponding to CuO disappear and only one peak at 520 cm^{-1} is observed (Fig. 1(b)), which may be due to the uniform immobilization of bulky uricase molecules on the surface of CuO thin films.

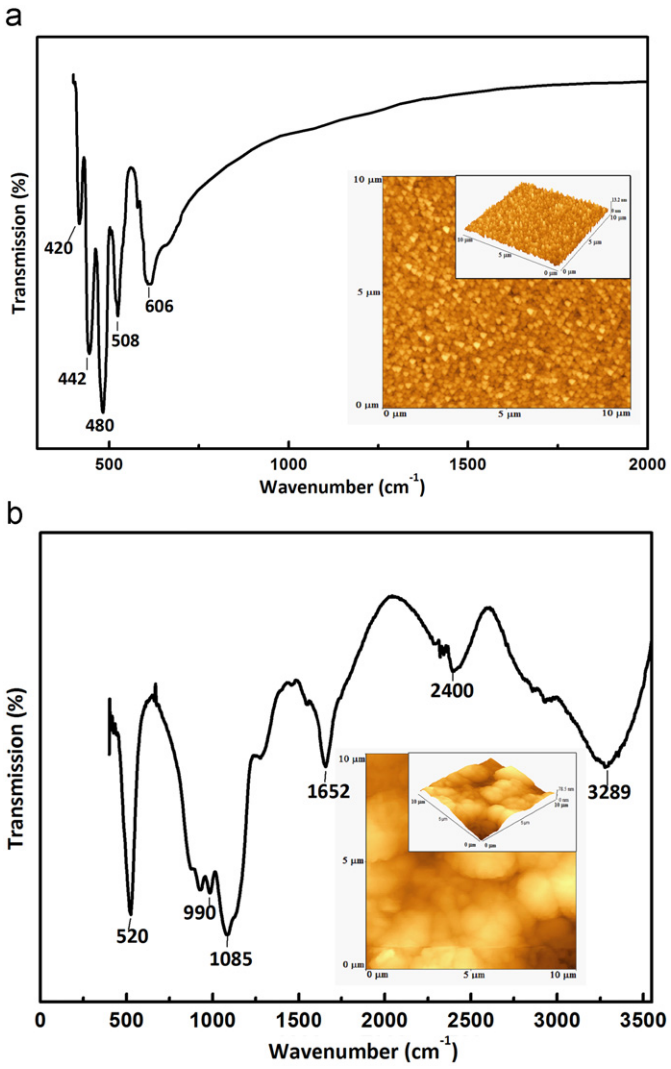

Fig. 1. FTIR spectra of (a) CuO/Pt/glass electrode and (b) uricase/CuO/Pt/glass bio-electrode. Inset shows the corresponding AFM micrographs along with their 3-D images.

3.3. AFM studies

The surface morphology of CuO/Pt/glass electrode in the presence and absence of uricase was characterized using atomic force microscopy (AFM) technique. Inset of Fig. 1(a) and (b) shows the AFM images of as-deposited CuO thin films before and after uricase immobilization, respectively. 3-dimensional scan of the respective electrodes are shown in their insets. AFM image of the as-deposited CuO thin film reveals the formation of rough surface morphology with uniformly distributed grains (~30 nm) and nanoporous morphology [inset (Fig. 1(a))] which is advantageous for enhanced enzyme loading. The average root mean square (rms) roughness of the film surface has been found to be about 6 nm. In the AFM micrograph of uricase/CuO/Pt bio-electrode [inset (Fig. 1(b))], presence of uniformly distributed globular structure (~1–3 μm) along with an increase in average rms roughness to ~36 nm indicates the successful immobilization of uricase on the surface of CuO thin film (Bhambi et al., 2010). The formation of globular structure may be attributed to the fact that the enzymes tend to undergo agglomeration upon immobilization, thus resulting in the formation of globules. The formation of globular structure on enzyme immobilization is in agreement to that reported by various workers for other biomolecules as well (Ram et al., 2001; Dhand et al., 2009).

3.4. Amperometric response

Inset of Fig. 2 gives the cyclic voltammetric (CV) curve obtained for Pt/glass, CuO/Pt/glass and uricase/CuO/Pt/glass electrodes in the PBS solution without any mediator. It can be clearly seen from the fig. that no redox peak is observed in the CV curve for Pt/glass electrode in PBS solution because Pt does not have any redox couple of its own and in the absence of any mediator in the electrolyte solution, it does not show any redox peak. On the other hand, the CV spectra of CuO/Pt/glass electrode, clearly show well defined redox peaks in a mediator-free PBS buffer which is attributed to the valence transformation of copper from Cu^{1+} to Cu^{2+} and vice-versa, (Xie and Huber, 1991) thus resulting in accelerated electron transfer. Also, the peak current for CuO/Pt/glass electrode is found to be much higher (3.31 mA) as compared to that of bare Pt/glass (0.07 mA) indicating that CuO film provides good electrocatalytic properties, and CuO thin film matrix sets up the reversible redox property in the electrode and serves as the electron transfer channel. The value of peak oxidation current obtained for CuO matrix was found to be much higher in comparison to that reported for other metal oxide matrices for biosensing such as NiO-chitosan (Singh et al., 2011), ZrO_2 (Das et al., 2010), ZnO (Saha et al., 2009a) etc. In order to understand this behavior, electrical properties (carrier concentration and mobility) of the CuO thin film were measured using the Van der Pauw hall effect measurements. It was observed that CuO thin film exhibits a p-type conductivity along with hole mobility of 18 $cm^2 V^{-1} s^{-1}$ with a carrier density of 6.6×10^{17} cm^{-3}. The mobility of charge carriers was found to be much higher compared to reported values for other p-type metal oxides (Lee and Lai, 2009). Probably the large mobility of charge

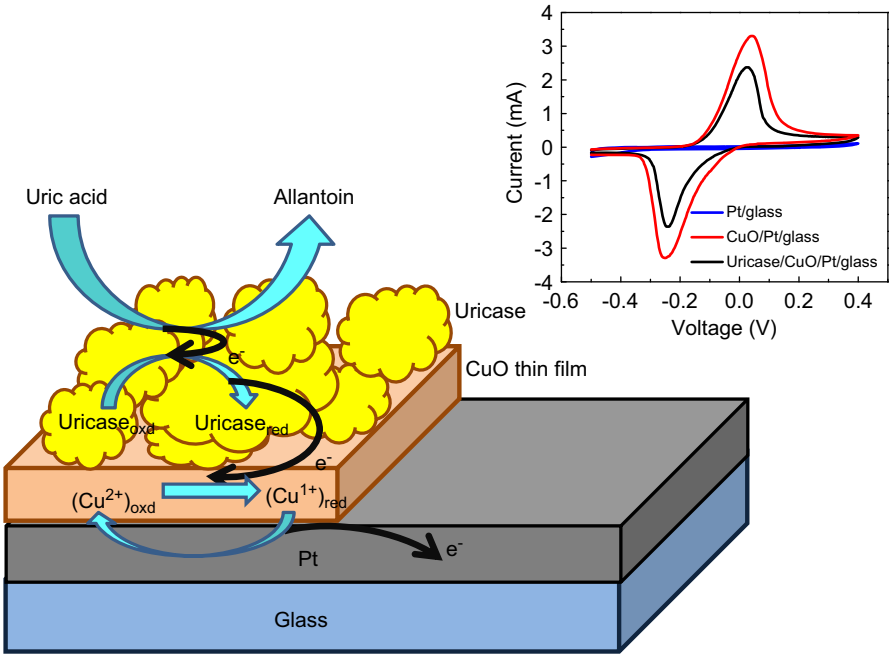

Fig. 2. Schematic of the electron exchange between uricase active center and CuO/Pt/glass electrode in the presence of uric acid. Inset shows the cyclic voltammetry response of Pt/glass electrode, CuO/Pt/glass electrode and Uricase/CuO/Pt/glass bio-electrode in a mediator free PBS solution.

carriers observed for CuO film in the present work is responsible for the excellent electron communication features of the electrode and thus contributes to the enhanced peak current in the CV spectra of CuO/Pt/glass electrode.

The magnitude of anodic and cathodic peak currents decreases on immobilization of uricase on the surface of the prepared electrode (anodic peak current = 2.4 mA). The observed decrease in peak current is owing to the formation of non-conducting layer of uricase enzyme on the electrode surface, which hinders the interfacial electron transfer. Since the activity of the enzyme (uricase) is highly sensitive to the variation of pH of the supporting buffer solution (PBS), the effect of pH on the response of the bio-electrode was investigated. The peak oxidation current of the uricase/CuO/Pt/glass bio-electrode was measured in a PBS solution of varying pH (Supplementary Fig. 2). The response increased when the pH increased from 6.0 to 7.0 and it started to decline for further increase in pH value till 8.0, indicating that the uricase exhibit maximum activity at a pH of 7.0. So, pH 7.0 was chosen to be the optimum pH for the entire work.

3.4.1. *Effect of scan rate*

In order to investigate the effect of scan rate on the response of the bio-electrode, cyclic voltammograms of uricase/CuO/Pt/glass bio-electrode as a function of scan rate (ν) varying from 70 to 150 mV/s were recorded and are shown in Fig. 3. It was found that as the scan rate increases, uricase oxidation and reduction peak current increases along with a gradual potential shift of the oxidation peak towards positive direction and reduction peak towards negative direction implying the quasi-reversibility (Saha et al., 2009a) of the system. Both the anodic (I_{pa}) and cathodic (I_{pc}) peak currents vary linearly with the square root of scan rate over the range (70–150 mV/s) (inset of Fig. 3), suggesting that the redox process of immobilized uricase follows kinetics controlled by diffusion. The linear regression equations fitted for both the peak anodic as well as cathodic currents are given as:

$$I_{pa} = 0.90599\nu^{1/2} - 6.21 \quad (r^2 = 0.9974 \text{ and S.D.} = 0.0160) \qquad (1)$$

$$I_{pc} = -0.86128\nu^{1/2} + 5.90455 \quad (r^2 = 0.9919 \text{ and S.D.} = 0.020) \qquad (2)$$

where, r is the regression coefficient and S.D. is the standard deviation. Value of regression coefficient close to 1 and small value of standard deviation indicate a good linear fit. The anodic peak potential (E_{pa}) was also found to vary linearly as a function of logarithm of scan rate and follows equation:

$$E_{pa} = 0.24745 \log\nu - 0.45702 \quad (r^2 = 0.9887 \text{ and S.D.} = 0.0093) \qquad (3)$$

An approximate estimation of the surface concentration (I^*) per unit area of the electroactive uricase for uricase/CuO/Pt/glass bioelectrode was made by using the Brown–Anson model (Bard and Faulkner, 2000) based on the following equation:

$$I_{pa} = \frac{n^2F^2I^*A\nu}{4RT}$$

where I_{pa} is the anodic peak current, n is the number of electrons exchanged per reactant molecule, F is the Faraday constant (96,485 C/mol), I^* is the surface coverage of the uricase/CuO/Pt/glass bioelectrode (mol cm^{-2}), A is surface area of the bio-electrode (0.25 cm^2), ν is scan rate, R is gas constant (8.314 J mol^{-1} K^{-1}), and T is the temperature (300 K). The estimated value of surface concentration of uricase/CuO/Pt/glass bioelectrode is about 1.73×10^{-5} mol/cm^2 which is greater in comparison to the corresponding value reported for other uricase bio-electrodes (Li and Lin, 2007). The increased value of I^* obtained in the present work confirms the efficient immobilization of uricase molecules on the electrode surface.

3.4.2. *Sensing response for uric acid*

The sensing response of the prepared biosensor (uricase/CuO/Pt/glass bio-electrode) was studied over the concentration range 0.05–1.0 mM of uric acid in mediator-free PBS (pH 7.0) solution. Concentration of uric acid (0.05–1.0 mM) is chosen so that it lies well beyond the physiological range (0.13–0.46 mM). The schematic of the biochemical reaction occurring at uricase/CuO/Pt/glass bio-electrode is shown in Fig. 2. Oxidation of uric acid in the presence of uricase produces allantoin. CuO directly accepts an electron from the active sites of reduced uricase (Fig. 2). On accepting an electron, CuO is reduced, which on re-oxidation produces an electron. The electrons generated as part of this

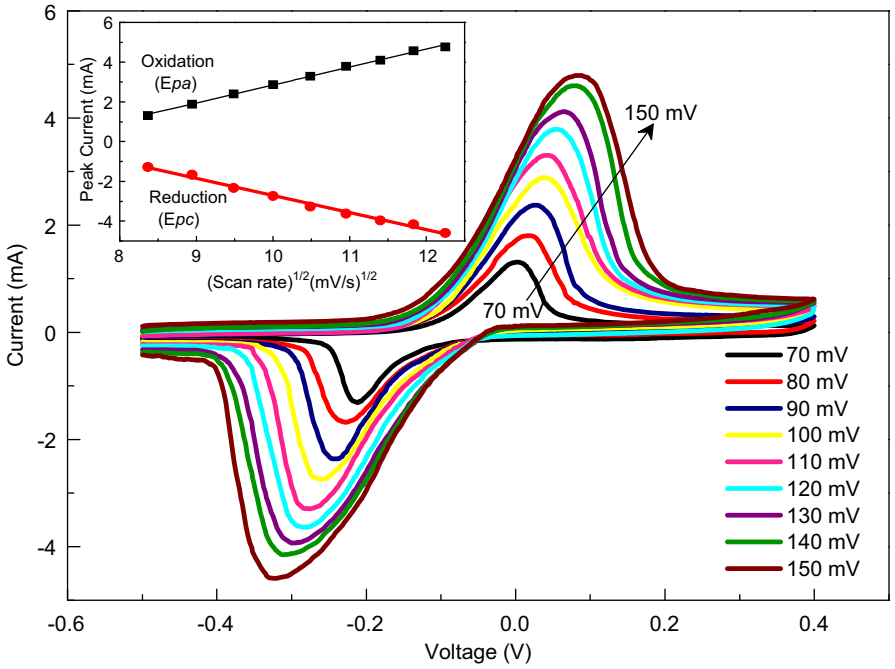

Fig. 3. CV spectra of uricase/CuO/Pt/glass bio-electrode at varying scan rates (70–150 mV/s). Inset shows the variation of the peak oxidation and reduction currents as a function of (scan rate)$^{1/2}$.

bio-chemical reaction are being captured by the electrode resulting in enhancement of the current. Fig. 4 shows the electrochemical sensing response of the biosensor as a function of uric acid concentration. Well-defined, stable and fast amperometric responses were observed for the prepared bio-electrode (uricase/CuO/Pt/glass) over the entire measured concentration of uric acid. The CuO thin film matrix serves as an efficient electron conducting channel in a mediator-less electrolyte due to its redox property as Cu is able to change reversibly from Cu^{1+} to Cu^{2+} under reducing conditions and vice versa. Thus CuO acts as a better matrix for electron transfer, over bio-oxygen, resulting in a peak at a relatively lower potential (0.1 V). It was observed that the amperometric response (oxidation peak current) increased with increasing uric acid concentration. The continuous rise in the oxidation current with increasing uric acid concentration is attributed to the release of more number of electrons in the catalytic oxidation of uric acid by uricase. In order to confirm the uricase catalyzed bioelectrocatalytical process in the present study, a control experiment was carried out in which sensing response for uric acid was also studied without immobilization of uricase on the surface of CuO/Pt/glass electrode. It is important to point out that no increase in oxidation and reduction currents were observed in the CV with increase in uric acid concentration from 0.05 mM to 1.0 mM. Thus, the performed control experiment confirmed that the increase in CV current observed in the biosensing reaction involving uricase/CuO/Pt/glass bio-electrode with varying uric acid concentrations is solely due to the bioelectrocatalytic oxidation of uric acid in presence of immobilized uricase.

The results indicate that the fabricated uricase/CuO/Pt/glass biosensor exhibit a good linearity in the peak oxidation current over a wide range of uric acid concentration (0.05–1.0 mM) with a linear regression equation:

$$\text{Peak current(mA)} = 2.701 \times \text{uric acid concentration (mM)} + 2.906 (r^2 = 0.992), \quad (4)$$

which is large enough for its application in physiological conditions. This further shows that the enzyme catalytic reaction of uricase is the first-order reaction. The sensitivity of the uricase/CuO/Pt/glass bio-electrode towards uric acid was about 2.7 mA(mM)$^{-1}$ in the range of 0.05–1.0 mM (inset (a) in Fig. 4) which is relatively better than those reported recently by various workers for uric acid biosensors (Ahuja et al., 2010; Chen et al., 2010). The lower detection limit (LDL) of the uric acid biosensor, calculated using the expression $3s_{y/x}$/sensitivity (Arora et al., 2011), where $s_{y/x}$ is the standard deviation, is found to be 0.14 mM at a signal-to-noise ratio of 3, which is attributed to high efficiency of electron transfer between the immobilized uricase and the Pt electrode via CuO thin film matrix. Furthermore, it is found that the uric acid biosensor prepared in the present work exhibited a fast response time i.e. it could achieve 95% of the steady signal within 4 s indicating a rapid oxidative process, which is much faster than those in similar determination by various workers using other matrices.

The value of Michaelis–Menten kinetic parameter (K_m) for the immobilized uricase was estimated from Hanes plot (graph between [uric acid concentration] and [uric acid concentration/current]), shown in the inset (b) of Fig. 4. The graph is found to be a straight line with regression coefficient $\sim > 0.99$.

The estimated value of K_m for prepared bio-electrode is about 0.12 mM which is much lower than the corresponding value reported by other workers for uric acid biosensors (Arora et al., 2009; Jiang et al., 2007; Zhang et al., 2007). The low value of K_m revealed the increased affinity of uricase/CuO/Pt/glass bio-electrode towards uric acid, thus, favoring electrochemical reaction. This is attributed to enhanced diffusion of uric acid through the surface of uricase/CuO/Pt/glass bio-electrode facilitated by a suitable biocompatible microenvironment provided by CuO thin film matrix and favorable conformational changes in the immobilized uricase on the matrix surface.

3.5. Photometric enzyme assay

UV–visible spectrophotometer studies have been performed to estimate the apparent enzyme activity of the uricase/CuO/Pt/glass bio-electrode. The difference between the initial and final absorbance value at a fixed wavelength (λ=500 nm) corresponding to

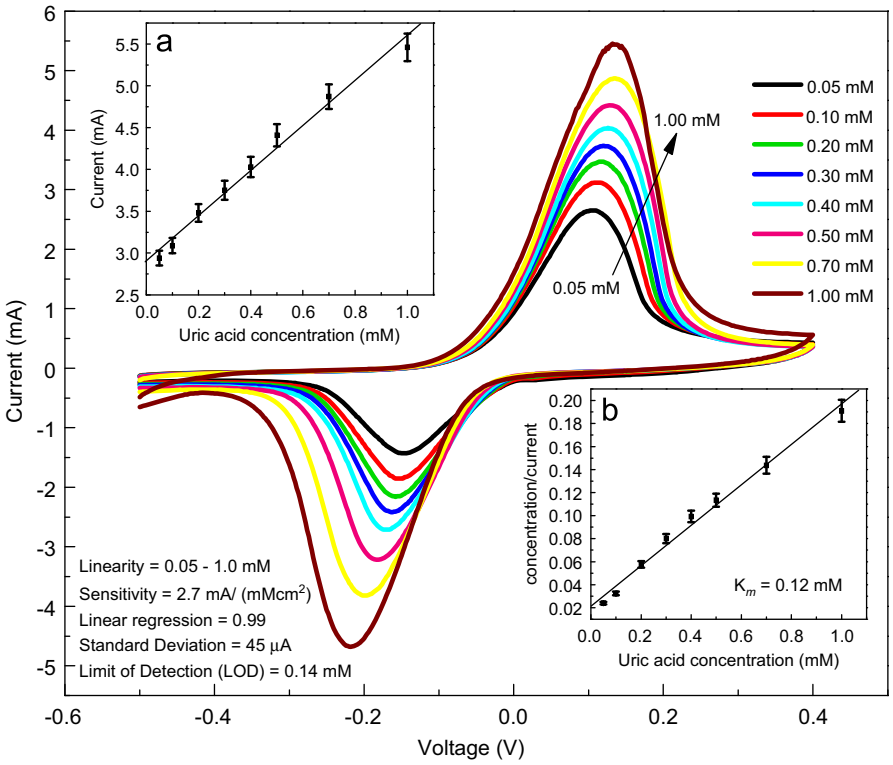

Fig. 4. Electrochemical response of uricase/CuO/Pt/glass bio-electrode with uric acid concentration (0.05–1.0 mM). Inset (a) shows the variation in oxidation peak current with uric acid concentration and (b) Hanes plot.

the absorption of o-dianisidine dye is recorded as a function of uric acid concentration and is shown in Fig. 5. The enzyme activity increases linearly with increase in uric acid concentration up to 0.5 mM and thereafter, saturates to a constant value (Fig. 5). The apparent enzyme activity, i.e. the amount of enzyme bound on the surface of the CuO matrix, has been estimated using the equation a_{app}^{enz} (U cm^{-2})=AV/εts, where A is the difference in absorbance of bio-electrode before and after incubation when saturation is achieved, V is the total volume (3.17 cm^3), ε is the millimolar extinction coefficient (7.5 for o-dianisidine at λ=500 nm), t is the reaction time (2 min) and s is the surface area (0.25 cm^2) of the bio-electrode (Saha et al., 2009a). The apparent enzyme activity for the uricase/CuO/Pt/glass bio-electrode was estimated to be 2.53×10^{-2} U cm^{-2} indicating that large units of uricase biomolecules are active on a unit surface area (1 cm^2) of the electrode. The value of enzyme activity estimated from the photometric assay does not agree with the surface concentration of ionic species calculated from amperometric measurements. The disagreement between the two values may be understood from the fact that the calculation of surface concentration provides the maximum surface coverage of the enzyme (uricase) on the surface of bio-electrode. Whereas, the value of enzyme activity, corresponds to the concentration of enzyme active sites participating in the bio-chemical reaction per unit time i.e. transfer of analyte (uric acid) from the buffer solution to the active sites of the immobilized uricase on the surface of sensing electrode. Similar kind of mismatch in the two values obtained from the amperometric and photometric study has also been reported (Matharu et al., 2009).

3.6. Shelf life of the uric acid biosensor

In order to investigate the bio-electrode stability for repeated usage over a period of time, the shelf life of the prepared uricase/CuO/Pt/glass bio-electrode has been studied by continuously monitoring the current response to a fixed concentration of uric acid (0.30 mM) at regular intervals of time (15 day) for around 4 months. The percent residual activity has been measured by assigning 100% activity observed in the initial stage (0 day). The variation in activity of the bio-electrode has been plotted in inset of Fig. 5 as a function of time. It has been found that immobilized uricase retains more than 90% of its activity even after 14 weeks when stored at 4 °C, indicating better stability of the CuO based bio-electrode. The results obtained in present study are promising compared to those reported by other workers for uric acid biosensors (Ali et al., 2011; Zhang et al., 2004; Zhang et al., 2006).

3.7. Selectivity of uric acid biosensor

In order to study the selectivity of the developed uric acid biosensor, a control experiment was performed in which the effect of interferants present in serum including glucose (5 mM), cholesterol (5 mM), urea (1 mM), ascorbic acid (0.1 mM) and lactic acid (0.5 mM) on its sensing response towards uric acid is studied. The experiment is carried out by taking a solution containing a 1:1 ratio of uric acid (0.10 mM) and the interferent in their normal physiological limits in the PBS solution and the observed variation in peak oxidation current with various interferants is shown in Supplementary Fig. 3. The two red-colored zones in the graph, brown and red, give the positive and negative errors, respectively in the measurement. The selectivity study suggests that the presence of interferants, like cholesterol, glucose, lactic acid, urea, and ascorbic acid, have a negligible effect on the performance of the uricase/CuO/Pt/glass bioelectrode toward sensing of uric acid. Thus, the prepared bio-electrode can be applied for the quantificational detection of uric acid in the presence of above interferents in normal concentrations also.

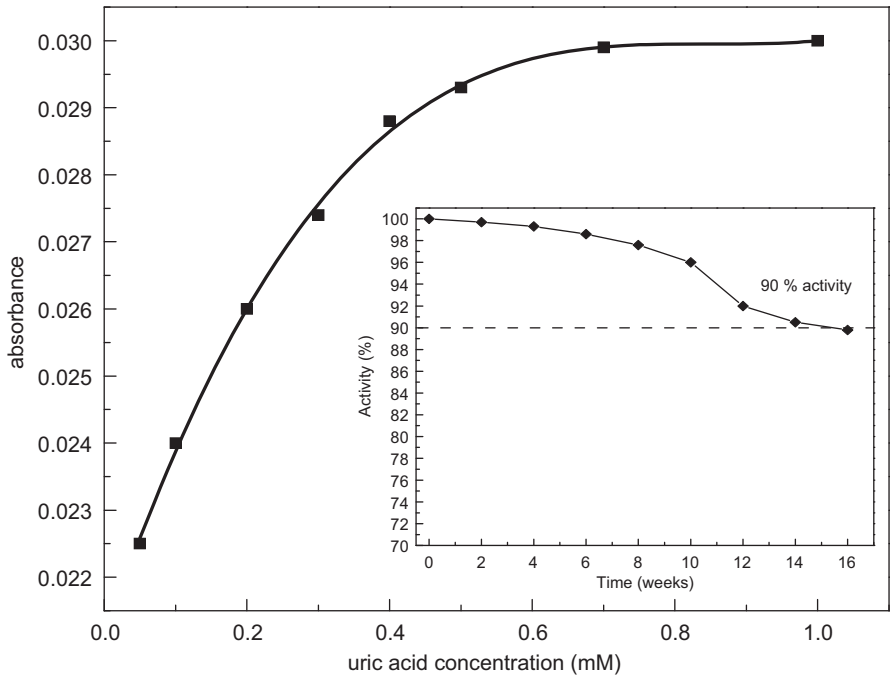

Fig. 5. Photometric assay of uricase/CuO/Pt/glass bio-electrode as a function of uric acid concentration. Inset shows the shelf life study of the uricase/CuO/Pt/glass bio-electrode.

Table 1
Determination and recovery of uric acid in human serum samples using the proposed biosensor.

Real sample (serum)	Concentration of uric acid measured (mM)		R.S.D. of developed biosensor ($n=6$) (%)	Spike (mM)	Concentration of uric acid detected (mM)	Recovery (%)	R.S.D. of developed biosensor ($n=6$) (%)
	Uricase/CuO/Pt/glass biosensor	Spectrophotometric method					
1	0.239	0.243	1.2	0.5	0.751	102.4	1.5
2	0.298	0.309	2.7	0.5	0.791	98.6	2.2
3	0.153	0.160	2.1	0.5	0.648	99	1.9
4	0.405	0.410	1.8	0.5	0.904	99.8	2.0
5	0.483	0.481	3.0	0.5	0.984	100.2	2.4
6	0.612	0.621	2.5	0.5	1.115	100.6	1.9

3.8. Determination of uric acid in real samples

To demonstrate the feasibility of the developed uricase/CuO/Pt/glass biosensor for the analysis of uric acid in human serum, 6 human serum samples were analyzed and the % recovery and precision were calculated for spiked samples. In order to obtain the uric acid concentration in real serum, CV analysis was performed to obtain the current response in the same way as for the uric acid solution and the uric acid concentration was interpolated from the calibration curve. To validate the accuracy of the fabricated uric acid biosensor, the content of uric acid in serum samples determined by the biosensor was compared with that measured by commercial spectrophotometric method in the laboratory. Table I summarizes the results obtained during the present investigation. The results indicate that the uric acid analyses in serum with the developed biosensor agreed well with the spectrophotometric data. Real samples were then spiked with known concentration (0.5 mM) of uric acid and the recovery tests for uric acid were performed. The amounts of added uric acid were then evaluated by using the proposed uric acid biosensor (Table 1). The recovery tests demonstrate that the developed uricase/CuO/Pt/glass biosensor is accurate and precise and the performance of the uricase/CuO/Pt/glass biosensor system is comparable with the commercially accepted methods.

Supplementary Table 1 displays the comparison of the analytical performance between the various reports on uric acid biosensors along with the proposed CuO matrix based biosensor. The advantage of the bio-electrode prepared in present work is clearly visible as most of the earlier work is based on complex electrode fabrication technology besides relatively lower sensing response for uric acid. The cross-linkers are generally used for immobilization of enzyme on the matrix surface. In order to overcome this, surprisingly, very little efforts have been made towards the exploitation of metal oxide thin films with higher iso-electric point. The prepared biosensor (uricase/CuO/Pt/glass) was found to exhibit a higher current sensitivity (2.7 mA/mM) and high affinity (lower $K_m \sim 0.12$ mM) towards uric acid without any mediator. The sensor shows good linearity over a broad range of 0.05–1.0 mM uric acid concentration, well beyond the physiological range. The enhanced response may be due to the presence of the rough surface of CuO matrix that results in higher activity of immobilized uricase molecules leading to their enhanced interaction with analyte along with the electrocatalytic activity of Cu^{1+}/Cu^{2+} redox couple making the electrode highly

sensitive without any external mediator. Also, the shelf life of the developed biosensor is much better than those reported in literature (Li and Lin, 2007; He et al., 2007) which may be attributed to the fact that the CuO thin film deposited by pulsed laser deposition is providing suitable microenvironment to the immobilized uricase to retain its bio-activity for a longer time.

Thus, we demonstrate that the developed uric acid biosensor fulfills the criteria (biocompatibility, linearity, sensitivity, specificity, accuracy, long-term stability) of in-vivo application in clinical practice. In addition, it is free from the toxic mediators and is capable of electron transfer without any external mediator and thus, can be employed for developing implantable biosensors. The development may be based on the silicon wafer based platinum microelectrode array where a thick layer of silicon dioxide is coated on a silicon substrate to isolate it from the metal layer subsequently deposited. The platinum counter electrode, a reference Ag/AgCl electrode, microdisc based working electrode and the bonding pads may be patterned using photolithography (Guiseppi-Elie et al., 2005) for the realization of an implantable biosensor (Supplementary Fig. 4).

4. Conclusion

CuO thin film has been identified as a promising matrix for realization of a reagentless uric acid biosensor. The CuO matrix with rough surface has been successfully utilized for the immobilization of the uricase, and efficiently exploited for uric acid biosensing based on the bioelectrocatalytic oxidation of uric acid by uricase. Presence of the redox species in the matrix enhances the charge transfer rate and provides a quassireversible system. The lower value of Michaelis–Menten constant (0.12 mM) proves that the CuO thin film matrix provides a platform in which the enzyme not only retains its bioactivity but maintains a confirmation. Moreover, the fabricated bio-electrode (uricase/CuO/Pt/glass) shows a fast and good linear response without any external mediator. Shelf life of the bio-electrode is found to be more than 14 weeks. Our results suggest that the prepared CuO thin film based bio-electrode has potential applications for the fabrication of reagentless integrated biosensor chip.

Acknowledgment

Authors are thankful to Department of Science and Technology (DST) for the financial support to carry out the proposed work. One of the authors (KJ) acknowledges UGC for fellowship and University of Delhi for teaching assistantship.

Appendix A. Supporting information

Supplementary data associated with this article can be found in the online version at http://dx.doi.org/10.1016/j.bios.2012.03.043.

References

Ahuja, T., Rajesh Kumar, D., Tanwar, V.K., Sharma, V., Biradar, A.M., Singh, N., 2010. Thin Solid Films 519, 1128–1134.
Ali, S.M.U., Alvi, N.H., Ibupoto, Z., Nur, O., Willandera, M., Danielsson, B., 2011. Sensors and Actuators B 152, 241–247.
Alkire, R.C., Kolb, D.M., Lipkowski, J., 2011. Bioelectrochemistry: Fundamentals, Applications and Recent Developments, Vol. 16. Wiley-VCH.
Arora, J., Nandwani, S., Bhambi, M., Pundir, C.S., 2009. Analytica Chimica Acta 647, 195–201.
Arora, K., Tomar, M., Gupta, V., 2011. Biosensors and Bioelectronics 30, 333–336.
Arslan, F., 2008. Sensors 8, 5492–5500.
Balamurunga, B., Mehta, B.R., 2001. Thin Solid Film 396, 90–96.
Bard, A.J., Faulkner, L.R., 2000. Electrochemical Methods: Fundamentals and Applications, 2nd Ed. Wiley, New York.
Bhambi, M., Sumana, G., Malhotra, B.D., Pundir, C.S., 2010. Artificial Cells, Blood Substitutes, and Immobilization Biotechnology 38, 178–185.
Cete, S., Yasar, A., Arslan, F., 2006. Artificial Cells, Blood Substitutes, and Immobilization Biotechnology 34, 367–380.
Chen, P.Y., Vittal, R., Nien, P.C., Liou, G.S., Ho, K.C., 2010. Talanta 8, 1145–1151.
Das, M., Sumana, G., Nagarajan, R., Malhotra, B.D., 2010. Applied Physics Letters 96, 133703.
Dhand, C., Solanki, P.R., Sood, K.N., Datta, M., Malhotra, B.D., 2009. Electrochemical Communications 11, 1482–1486.
Gilmartin, M.A.T., Hart, J.P., 1994. Analyst 119, 833–840.
Guiseppi-Elie, A., Brahim, S., Slaughter, G., Ward, K.R., 2005. IEEE Sensors Journal 5, 345–355.
He, J.B., Jin, G.P., Chen, Q.Z., Wang, Y., 2007. Analytica Chimica Acta 587, 337–343.
Jiang, Y., Wang, A., Kan, J., 2007. Sensors and Actuators B 124, 529–534.
Joint Committee on Powder Diffraction Standards, Diffraction Data File, No. 5-661, 1991, JCPDS International Center for Diffraction Data, Pennsylvania.
Kan, J., Pan, X., Chen, C., 2004. Biosensors and Bioelectronics 19, 1635–1640.
Kliche, K., Popovic, Z.V., 1990. Physical Review B 42, 10060.
Lee, Y.M., Lai, C.H., 2009. Solid State Electronics 53, 1116–1125.
Li, J., Lin, X.Q., 2007. Analytica Chimica Acta 596, 222–230.
Luo, Y.C., Do, J.S., Liu, C., 2006. Biosensors and Bioelectronics 22, 482–488.
Matharu, Z., Pandey, P., Pandey, M.K., Gupta, V., Malhotra, B.D., 2009. Electroanalysis 21, 1587–1596.
McAuley, C.B., Du, Y., Wildgoose, G.G., Compton, R.G., 2008. Sens. Actuators B 135, 230–235.
MedlinePlus: US National Library of Medicine, National Institutes of Health.
Perez, D.M., Ferrer, M.L., Mateo, C.R., 2003. Analytical Biochemistry 322, 238–242.
Ram, M.K., Bertoncello, P., Ding, H., Paddeu, S., Nicolini, C., 2001. Biosensors and Bioelectronics 16, 849–856.
Saha, S., Arya, S.K., Singh, S.P., Sreenivas, K., Malhotra, B.D., Gupta, V., 2009a. Analytica Chimica Acta 653, 212–216.
Saha, S., Arya, S.K., Singh, S.P., Sreenivas, K., Malhotra, B.D., Gupta, V., 2009b. Biosensors and Bioelectronics 24, 2040–2045.
Saha, S., Gupta, V., 2011. Journal of Applied Physics 110, 064904.
Saha, S., Gupta, V., Sreenivas, K., Tan, H.H., Jagadish, C., 2010. Applied Physics Letters 97, 133704.
Singh, J., Kalita, P., Singh, M.K., Malhotra, B.D., 2011. Applied Physics Letters 98, 123702.
Singh, S.P., Arya, S.K., Pandey, P., Malhotra, B.D., Saha, S., Sreenivas, K., Gupta, V., 2007. Applied Physics Letters 91, 063901.
Vaseem, M., Umar, A., Kim, S.H., Hahn, Y.B., 2008. Journal of Physical Chemistry C 112, 5729–5735.
Wang, X., Hu, C., Liu, H., Du, G., He, X., Xi, Y., 2010. Sensors and Actuators B 144, 220–225.
Wang, X., Yao, Y., Zhang, J., Zhu, Z., Zhu, J., 2008. Sensors and Materials 20, 111–121.
Wang, X.Y., Hagiwara, T., 2007. Uchiyama, S. Analytica Chimica Acta 1, 41–46.
Xie, Y., Huber, C.O., 1991. Analytical Chemistry 63, 1714–1719.
Zhang, F., Li, C., Li, X., Wang, X., Wan, Q., Xian, Y., Jin, L., Yamamoto, K., 2006. Talanta 68, 1353–1358.
Zhang, F., Wang, X., Ai, S., Sun, Z., Wan, Q., Zhu, Z., Xian, Y., Jin, L., Yamamoto, K., 2004. Analytica Chimica Acta 519, 155–160.
Zhang., Y., Wen., G., Zhou., Y., Shuang., S., Dong, C., Choi, M.M.F., 2007. Biosensors and Bioelectronics 22, 1791–1797.